(19) In addition to the local data-reduction program ENXDR, the programs used included full-matrix least-squares and Fourier programs, ABSCOR, a numerical method absorption correction program which applies a Gaussian grid to the crystal, and Johnson's ORTEP. All calculations were carried out on a PDP 11/45 computer. Atomic scattering factors were taken from "International Tables for X-ray Crystallography", Vol. IV, Kynoch Press, Birmingham, England, 1974.
(20) H. J. Peresie and J. A. Stanko, *Chem. Commun.*, 1674 (1970).
(21) M. T. Flood, R. F. Ziolo, J. E. Earley, and H. B. Gray, *Inorg. Chem.*, **12**, 2153 (1973).
(22) F. C. March and G. Ferguson, *Can. J. Chem.*, **49**, 3590 (1971).
(23) S. S. Isied and H. Taube, *Inorg. Chem.*, **15**, 3070 (1976).
(24) J. K. Beattie, C. L. Raston, and A. H. White, *J. Chem. Soc., Dalton Trans.*, 1121 (1977).

Contribution from the Department of Chemistry, Indian Institute of Technology, Madras 600036, India, and Central Instruments and Services Laboratory, Indian Institute of Science, Bangalore 560012, India

Crystal and Molecular Structure of Two Crystalline Modifications of Bis[1-methyl-3-(2-chloro-6-methylphenyl)triazine 1-oxidato]nickel(II), NiBPT—a Bis Chelate with a Five-Membered Ni–N–O Ring

M. V. RAJASEKHARAN,[1] K. I. VARUGHESE,[2] and P. T. MANOHARAN*[1]

Received August 23, 1978

The title compound is obtained in two different crystalline modifications. The green elongated parallelepiped crystals obtained from acetone solutions belong to the monoclinic space group $P2_1/a$ with $Z = 4$, $a = 14.306$ (3) Å, $b = 7.858$ (1) Å, $c = 18.605$ (3) Å, $\beta = 103.72$ (3)°, $d_{calcd} = 1.489$ g/cm^3, and $d_{measd} = 1.50$ g/cm^3. A benzene solvate, NiBPT·C_6H_6, belonging to the space group $P\bar{1}$ is obtained from benzene solutions and has $Z = 1$, $a = 7.9637$ (9) Å, $b = 9.246$ (2) Å, $c = 9.999$ (2) Å, $\alpha = 63.93$ (1)°, $\beta = 77.44$ (1)°, $\gamma = 68.57$ (1)°, $d_{calcd} = 1.442$ g/cm^3, and $d_{measd} = 1.42$ g/cm^3. The structures of both crystals were determined by using three-dimensional diffractometer data. In the case of NiBPT, full-matrix least-squares refinement using 2731 reflections having $I > 2\sigma(I)$ led to a conventional R value of 0.071. For NiBPT·C_6H_6 the refinement using 1523 reflections having $I > 3\sigma(I)$ converged to an R value of 0.032. The coordination in the NiN_2O_2 moiety is strictly planar in both modifications with Ni–O and Ni–N distances of 1.849 (4) and 1.846 (6) Å, respectively, and a N–Ni–O angle of 83.4 (2)°. (The values are averaged over the two structure determinations. The root-mean-square value of the esd's in individual measurements is given in parentheses.) The benzene molecule in the solvated crystal is situated too far from the nickel atom to have any appreciable interaction with it. The analogous cobalt complex, CoBPT, is shown to be isomorphous with NiBPT.

Introduction

Aromatic triazine 1-oxides, having the general formula Ar—NH—N=N(R)→O, where Ar is a phenyl or substituted phenyl group and R is an alkyl or aryl group, are potentially bidentate ligands which are known to form both bis and tris chelate complexes with various metal ions.[3] The coordination geometry and magnetic properties of the bis chelates are extremely sensitive to the number and nature of the substituents on the aromatic ring. Unsubstituted and methyl-substituted complexes of cobalt, for example, are not stable in air and could not be isolated.[3a] When Ar is *o*-C_6H_4X, where X = F, Cl, Br, OCH_3, OC_2H_5, or SCH_3, the ligand forms pseudooctahedral complexes involving a weak coordination of the halo group, while the iodo-substituted complex appears to be planar ($\mu_{eff} = 2.1\ \mu_B$) in the solid state and pseudooctahedral in solution ($\mu_{eff} = 4.4\ \mu_B$ in benzene solution).[3e] Disubstituted ligands with substituents at 2- and 6-positions form predominantly planar complexes.[3f] We had chosen one such complex, viz., CoBPT, for investigation as part of our more general project on the electronic structure of low-spin cobalt(II) complexes. In the course of our electron paramagnetic resonance (EPR) studies on this complex, it was felt that the interpretation of the single-crystal spectra and the analysis of the magnetic parameters would be greatly facilitated by a knowledge of the crystal structure of the corresponding isomorphous nickel complex, which was used as the host lattice for EPR measurements. In addition, we were interested in verifying an earlier hypothesis[4] regarding the weak coordination of the chlorine atom, which was suggested to be responsible for the large electric field gradient at the cobalt nucleus which manifested itself as a large quadrupole term in the spin Hamiltonian. In fact, such a weak chloro coordination had been established by crystal structure determination[5] in a similar cobalt complex, bis[1-methyl-3-(*o*-chlorophenyl)triazine 1-oxidato]cobalt(II) (CoBPTH).

Even though the crystal structure investigation was taken up with the above-mentioned objectives in mind, we found in the course of our work that the structure of the nickel complex is interesting in its own right. While the literature on the structure and stereochemistry of bis chelate complexes of the type

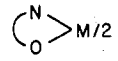

is quite prolific, they are mostly confined to systems with six-membered chelate rings.[6] Detailed structural data on five-membered ring complexes are limited to a few copper complexes,[7] even though a large number of such complexes have been characterized by other methods.[6] Hence the present structural report is believed to be of general interest in relation to the stereochemistry of bis chelate metal complexes.

NiBPT crystallizes in two crystalline modifications. A monoclinic form is obtained from most solvents such as chloroform, acetone, etc., while a triclinic modification results from benzene solutions. The latter modification turned out to be a benzene solvate containing weakly bound benzene in the lattice. These crystals rapidly lose benzene on standing and become powdery. A thermogravimetric analysis showed a weight loss corresponding to 1 mol of benzene. The crystal structures of both types of crystals are discussed in this report.

Experimental Section

Bis[1-methyl-3-(2-chloro-6-methylphenyl)triazine 1-oxidato]-nickel(II) was prepared as previously reported.[3d,f] Crystals of NiBPT suitable for X-ray work were obtained in the form of elongated parallelepipeds by slow evaporation of an acetone solution. Single crystals of NiBPT·C_6H_6 were obtained by slow evaporation of a

0020-1669/79/1318-2221$01.00/0

Table I. Crystal Data for NiBPT

formula: $NiC_{16}H_{18}N_6O_2Cl_2$	$V = 2031.8$ Å^3
fw: 455.6	λ: 0.710 69 Å
monoclinic	μ(Mo Kα) = 12.37 cm^{-1}
space group: $P2_1/a$	$d_{measd} = 1.50$ g cm^{-3}
$a = 14.306$ (3) Å	$d_{calcd} = 1.489$ g cm^{-3}
$b = 7.858$ (1) Å	$Z = 4$
$c = 18.605$ (3) Å	$F(000) = 234$
$\beta = 103.72$ (3)°	cryst size: 0.5 × 0.3 × 0.3 mm

Table II. Crystal Data for $NiBPT \cdot C_6H_6$

formula: $NiC_{16}H_{18}N_6O_2Cl_2 \cdot C_6H_6$	$V = 614.20$ Å^3
fw: 533.6	λ: 0.710 69 Å
triclinic	μ(Mo Kα) = 10.36 cm^{-1}
space group: $P\bar{1}$	$d_{measd} = 1.42$ g cm^{-3}
$a = 7.9637$ (9) Å	$d_{calcd} = 1.442$ g cm^{-3}
$b = 9.246$ (2) Å	$Z = 1$
$c = 9.999$ (2) Å	$F(000) = 276$
$\alpha = 63.93$ (1)°	cryst size: 0.5 × 0.3 × 0.3 mm
$\beta = 77.44$ (1)°	
$\gamma = 68.57$ (1)°	

benzene solution. Since the crystals rapidly lose benzene on standing, they were sealed in Lindemann glass capillary tubes with a tiny droplet of benzene. Sealed this way, the crystals do not lose benzene and were found to be stable for an indefinitely long period.

Crystal data of both NiBPT and $NiBPT \cdot C_6H_6$ are given in Tables I and II.

X-ray Data Collection and Reduction for NiBPT. Preliminary Weissenberg photographs (Cu Kα) showed Laue symmetry $2/m$. Systematic absences $h0l$ for $h = 2n + 1$ and $0k0$ for $k = 2n + 1$ unambiguously determine the space group as $P2_1/a$ (equivalent positions; $\pm(x, y, z)$; $\pm(x + {}^1/_2, {}^1/_2 - y, z)$). The intensity data were collected on a computer-automated Enraf-Nonius (CAD-4) diffractometer. The crystal was mounted with the b axis coincident with the spindle (φ) axis. Unit cell parameters were obtained by a least-squares fit to the θ values measured for 20 strong reflections chosen from diverse regions of reciprocal space by using the automatic centering routine supplied with the instrument. Intensities were measured by using a moving crystal, moving counter scan technique with graphite-monochromated Mo Kα radiation. The scan width for each reflection was $1.0 + 0.2 \tan\theta$ for the peak, and one-fourth of this value on either side for the background. A dispersion factor was added to compensate for the $K\alpha_1$–$K\alpha_2$ splitting at high angles. Variable scan speed was used, and whenever the counting rate exceeded 50 000 counts/s, a zirconium attenuator was automatically introduced. Three standard reflections from different regions of reciprocal space were measured after every 50 reflections. They remained essentially constant through the entire period of data collection.

The raw data were corrected for background, variable scan speed, attenuation factor, and Lorentz and polarization effects. No absorption correction was applied. From the stated dimensions of the crystal we estimated that the neglect of absorption will not affect any F_o by more than 3%. An estimated standard deviation in each structure factor was calculated from the formula

$$\sigma(F) = F\{[(I + \sigma(I))^{1/2} - I^{1/2}]^2/I + (\sigma(f)/2f)^2\}^{1/2}$$

where f is the attenuation factor and $\sigma(f)$ is its standard deviation. The standard deviation $\sigma(I)$ in the net count is given by $\{NC + 2(LB + RB)\}^{1/2}$ where NC is the total integrated peak count and LB and RB are the two background counts.

Of the 3681 unique reflections measured within a sphere of radius $(\sin\theta)/\lambda = 0.594$ Å^{-1}, 950 had $I \leq 2\sigma(I)$, and they were excluded from further calculation and refinement.

Solution and Refinement of the Structure.[8] The structure was solved by standard Patterson and Fourier methods. A three-dimensional Patterson syntheses using 2000 reflections was used to locate the nickel atom. A Fourier map phased on the position of the nickel atom and including all the observed reflections revealed the position of the two chlorine atoms. Three further successive three-dimensional Fourier syntheses revealed the positions of all remaining nonhydrogen atoms.

Refinement was carried out by using the full-matrix least-squares method. The function minimized was $\sum w(|F_o| - |F_c|)^2$. Anisotropic thermal parameters were assigned to all the nonhydrogen atoms. Three initial cycles of isotropic refinement using the Hughes weighting scheme ($w = (4F_{min})^2/F^2$ for $F \geq 4F_{min}$; otherwise $w = 1$) reduced the conventional R factor ($R_1 = \sum||F_o| - |F_c||/\sum|F_o|$) to 0.140. At this stage anisotropic thermal parameters were introduced, and the weighting scheme was changed to $w = 1/\sigma^2(F)$. Four cycles of full-matrix refinement varying only the parameters of the nickel atom and half the remaining molecule at a time reduced the R factor to 0.085. At this stage a difference map was computed. Twelve methyl hydrogens could be located from this map. The positions of the phenyl hydrogens were estimated from chemical knowledge and were fixed each at a distance of 1.0 Å from the respective carbon atoms. They were assigned isotropic thermal parameters of the same magnitude as those of the carbon atoms to which they were attached. Two cycles of anisotropic refinement varying the parameters of all the nonhydrogen atoms coverged with $R_1 = 0.071$ and the weighted residual factor $R_2 = \{\sum w(|F_o| - |F_c|)^2/\sum wF_o^2\}^{1/2} = 0.084$. For the final refinement cycle the corrections to all the parameters were less than 0.3 times their respective standard deviations. A difference map calculated at this stage was free of features above 0.6 e/Å^3. A total of 2731 reflections were included in the refinement, and the total number of parameters varied was 244.

Final least-squares atomic parameters for nonhydrogen atoms with estimated standard deviations derived from the inverse matrix are given in Table III(a). The hydrogen atom parameters (Table III(b)) as well as a listing of observed and calculated structure factor amplitudes are available.[9] In the listing the F_o values are scaled by a factor of 2.648.

X-ray Data Collection and Reduction for $NiBPT \cdot C_6H_6$. Preliminary Weissenberg photographs showed triclinic symmetry, implying that the space group is either $P1$ or $P\bar{1}$. Approximate unit cell parameters were calculated from zero-layer and first-layer Weissenberg pictures taken across the needle axis of the crystal which was chosen as the a axis of the triclinic unit cell.

The intensity data were collected on a computer-automated Enraf-Nonius (CAD-4) diffractometer. A freshly prepared crystal sealed in a Lindemann capillary tube was mounted with the crystallographic a axis coincident with the spindle (φ) axis. Refined unit cell parameters were obtained as before by centering 20 strong reflections. The procedure used for intensity measurement was essentially the same as in the case of the previous crystal except that a constant scan speed of 6.1°/min was used for all reflections. Four control reflections were measured after every 50 reflections to monitor crystal and electronic stability. The crystal was found to be highly stable, and no decrease in intensities of the control reflections was observed.

The raw data were directly reduced to a set of relative structure factors, and estimated standard deviations were assigned to them as described for the case of NiBPT. No absorption correction was applied. From the stated dimensions of the crystal we estimated that the neglect of absorption will not affect any structure factor amplitude by more than 3%.

Of the 1659 unique reflections measured within a sphere of radius $(\sin\theta)/\lambda = 0.537$ Å^{-1}, 136 reflections were found to have $I \leq 3\sigma(I)$, and they were excluded from further calculations and refinement.

Solution and Refinement of the Structure.[8] The structure was solved and refined on the assumption of space group $P\bar{1}$ with the Ni atom located at a center of symmetry. The position $({}^1/_2, {}^1/_2, {}^1/_2)$ was assigned to it, and the structure was solved by three successive three-dimensional Fourier syntheses. The free benzene molecule was located as centered at $(0, 0, {}^1/_2)$.

The refinement was carried out by using the full-matrix least-squares method. The function minimized was $\sum w(|F_o| - |F_c|)^2$. Weights were assigned to the structure factors based on their standard deviations ($w = 1/\sigma^2(F)$). Anisotropic thermal parameters were used for all nonhydrogen atoms. Three cycles of initial isotropic refinement converged to a conventional R value (R_1) of 0.119. Two cycles of anisotropic refinement were carried out which lowered the R factor to 0.057. At this stage all the hydrogen atoms were located from a difference map at their expected positions. Three cycles of anisotropic refinement including all the hydrogen atoms with isotropic thermal parameters were computed. The R value at this stage was 0.034. One final cycle was carried out by varying only the parameters of the nonhydrogen atoms. The final conventional and weighted residual factors are, respectively, $R_1 = 0.032$ and $R_2 = 0.047$. For the final refinement cycle, the corrections to all parameters were less than 0.3 times their respective standard deviations. A difference map computed at this stage was free of features above 0.33 e/Å^3. A total of 1523

Table III(a). Fractional Atomic Coordinates ($\times 10^4$) and Thermal Parameters ($Å^2$) for Nonhydrogen Atoms[a] in NiBPT

atom	x	y	z	B_{11}	B_{22}	B_{33}	B_{12}	B_{13}	B_{23}
Ni	1150 (1)	425 (1)	2448 (1)	4.17 (7)	2.03 (4)	3.27 (0)	−0.04 (4)	2.01 (0)	0.06 (5)
Cl	595 (2)	2091 (3)	284 (1)	5.41 (15)	6.15 (17)	6.79 (13)	0.48 (13)	1.51 (10)	0.62 (11)
O	798 (4)	−1820 (6)	2233 (3)	5.95 (38)	3.14 (27)	4.05 (26)	−1.22 (26)	2.91 (30)	−0.62 (22)
N(1)	1086 (5)	−2312 (8)	1630 (4)	5.95 (46)	2.49 (32)	3.92 (39)	−0.57 (30)	1.91 (30)	−0.23 (28)
N(2)	1553 (5)	−1293 (8)	1303 (3)	5.10 (38)	1.93 (29)	3.66 (39)	−0.57 (26)	1.81 (30)	−0.45 (28)
N(3)	1664 (5)	228 (8)	1636 (3)	4.25 (38)	2.40 (29)	3.40 (26)	−0.17 (26)	1.51 (30)	−0.11 (28)
C(1)	2224 (6)	1358 (9)	1300 (4)	4.25 (46)	2.22 (34)	3.01 (39)	−0.57 (30)	2.31 (40)	−0.68 (28)
C(2)	1819 (6)	2244 (10)	677 (4)	3.86 (46)	3.09 (39)	3.53 (39)	−0.04 (34)	1.81 (30)	−0.11 (34)
C(3)	2339 (7)	3383 (11)	339 (5)	5.49 (54)	3.78 (49)	5.62 (52)	0.57 (39)	3.11 (50)	1.19 (39)
C(4)	3321 (8)	3509 (13)	654 (6)	5.72 (61)	5.78 (59)	6.27 (65)	−1.18 (48)	3.42 (50)	0.97 (45)
C(5)	3748 (7)	2618 (13)	1277 (6)	4.17 (54)	5.63 (59)	5.88 (52)	−0.70 (43)	1.91 (50)	−0.68 (45)
C(6)	3205 (6)	1543 (11)	1625 (5)	4.09 (46)	3.24 (41)	4.70 (52)	−0.39 (34)	2.01 (40)	−0.97 (34)
C(7)	3704 (5)	541 (10)	2348 (4)	2.32 (38)	4.12 (41)	2.87 (39)	0.04 (34)	−0.40 (30)	0.80 (34)
C(8)	832 (7)	−4052 (10)	1353 (5)	7.34 (61)	2.59 (41)	5.23 (52)	−1.09 (39)	2.01 (50)	−1.02 (34)
Cl′	1979 (3)	−393 (4)	4674 (2)	9.27 (23)	9.34 (22)	7.32 (13)	1.75 (17)	1.11 (20)	0.34 (17)
O′	1492 (4)	2679 (6)	2644 (3)	5.49 (30)	1.78 (22)	4.05 (26)	−0.87 (21)	2.91 (30)	−0.45 (22)
N(1′)	1194 (5)	3167 (8)	3241 (4)	5.33 (38)	2.82 (34)	3.27 (26)	−0.35 (30)	1.91 (30)	−0.45 (28)
N(2′)	761 (5)	2164 (8)	3593 (3)	4.64 (38)	1.80 (29)	3.66 (26)	0.17 (26)	1.91 (30)	0.23 (22)
N(3′)	647 (5)	622 (8)	3272 (3)	4.87 (38)	1.98 (29)	3.27 (26)	−0.04 (26)	2.11 (30)	0.00 (22)
C(1′)	270 (7)	−568 (10)	3702 (5)	5.41 (54)	2.52 (37)	3.92 (39)	0.96 (39)	3.22 (40)	0.28 (34)
C(2′)	804 (7)	−1113 (11)	4373 (5)	4.94 (54)	3.56 (44)	4.05 (39)	1.00 (39)	2.11 (40)	−0.45 (34)
C(3′)	456 (9)	−226 (12)	4816 (5)	9.73 (77)	3.68 (49)	4.57 (39)	2.49 (52)	4.42 (60)	1.31 (39)
C(4′)	−478 (10)	−2869 (12)	4543 (7)	9.81 (84)	3.04 (49)	6.79 (65)	0.74 (52)	4.82 (70)	1.14 (45)
C(5′)	−1008 (8)	−2398 (12)	3873 (6)	7.80 (69)	3.63 (49)	7.58 (65)	−0.26 (48)	5.02 (60)	0.45 (45)
C(6′)	−676 (7)	−1222 (11)	3415 (6)	5.87 (61)	3.36 (44)	7.19 (65)	−0.57 (39)	5.02 (50)	−0.85 (39)
C(7′)	−1308 (5)	−638 (9)	2664 (4)	1.24 (30)	2.52 (34)	3.40 (39)	−0.35 (36)	0.40 (30)	0.80 (28)
C(8′)	1390 (8)	4944 (10)	3480 (5)	9.35 (69)	2.47 (44)	3.66 (39)	0.09 (39)	1.91 (50)	−0.23 (34)

[a] The form of the anisotropic thermal parameter is $\exp[-1/4(B_{11}h^2a^{*2} + B_{22}k^2b^{*2} + B_{33}l^2c^{*2} + 2B_{12}hka^*b^* + 2B_{13}hla^*c^* + 2B_{23}klb^*c^*)]$.

Table IV(a). Fractional Atomic Coordinates ($\times 10^4$) and Thermal Parameters ($Å^2$) for Nonhydrogen Atoms[a] in NiBPT·C_6H_6

atom	x	y	z	B_{11}	B_{22}	B_{33}	B_{12}	B_{13}	B_{23}
Ni	5000	5000	5000	2.01 (2)	3.37 (2)	2.02 (3)	−1.33 (0)	−0.16 (0)	−0.54 (0)
Cl	3057 (1)	4934 (1)	9298 (1)	5.71 (4)	6.34 (2)	5.59 (3)	−2.41 (2)	0.90 (2)	−3.26 (2)
O	7014 (2)	5366 (2)	5251 (1)	2.67 (6)	4.22 (4)	2.22 (6)	−1.99 (4)	−0.27 (5)	−0.34 (5)
N(1)	7468 (2)	4428 (2)	6684 (2)	2.49 (6)	4.02 (7)	2.47 (6)	−1.45 (4)	−0.48 (5)	−0.74 (5)
N(2)	6533 (2)	3501 (2)	7625 (2)	2.63 (6)	3.87 (7)	2.57 (6)	−1.61 (4)	−0.27 (5)	−0.68 (5)
N(3)	5204 (2)	3559 (2)	6997 (1)	2.30 (6)	3.75 (7)	2.51 (6)	−1.71 (4)	−0.27 (5)	−0.65 (5)
C(1)	4053 (2)	2613 (2)	8064 (2)	2.12 (6)	3.60 (7)	2.12 (6)	−1.40 (7)	−0.48 (5)	−0.11 (5)
C(2)	3004 (2)	3130 (2)	9177 (2)	2.54 (6)	4.25 (9)	2.57 (6)	−1.33 (7)	−0.34 (5)	−0.74 (5)
C(3)	1911 (2)	2218 (3)	10231 (2)	2.60 (8)	5.92 (12)	2.89 (9)	−1.45 (7)	−0.16 (5)	−0.85 (8)
C(4)	1859 (3)	780 (3)	10155 (2)	3.13 (8)	5.99 (7)	3.44 (9)	−2.59 (9)	−0.19 (7)	−0.08 (8)
C(5)	2872 (3)	269 (2)	9041 (2)	3.98 (8)	4.52 (9)	3.95 (9)	−2.38 (7)	−0.98 (7)	−0.31 (8)
C(6)	3983 (2)	1172 (2)	7969 (2)	2.76 (8)	4.02 (7)	2.73 (6)	−1.80 (7)	−0.72 (5)	−0.37 (5)
C(7)	5139 (3)	558 (2)	6770 (2)	3.79 (8)	3.70 (7)	3.60 (9)	−1.40 (7)	−0.37 (7)	−1.44 (8)
C(8)	8981 (2)	4618 (3)	7106 (2)	3.04 (8)	6.02 (9)	3.37 (9)	−2.52 (7)	−0.53 (7)	−1.25 (8)
C(B1)	−772 (3)	1733 (3)	4399 (3)	4.35 (10)	4.95 (12)	6.75 (12)	−1.99 (9)	−1.11 (10)	−2.52 (11)
C(B2)	399 (4)	980 (3)	5501 (3)	6.67 (15)	6.54 (14)	6.71 (16)	−3.74 (11)	1.27 (13)	−4.02 (11)
C(B3)	1169 (3)	−766 (3)	6121 (3)	5.43 (13)	6.39 (14)	5.56 (12)	−2.95 (11)	0.21 (10)	−2.38 (11)

[a] The form of the anisotropic thermal parameter is $\exp[-1/4(B_{11}h^2a^{*2} + B_{22}k^2b^{*2} + B_{33}l^2c^{*2} + 2B_{12}hka^*b^* + 2B_{13}hla^*c^* + 2B_{23}klb^*c^*)]$.

reflections were included in the refinement, and the total number of parameters was 199.

Final least-squares atomic parameters for the nonhydrogen atoms with estimated standard deviations derived from the inverse matrix are given in Table IV(a). The hydrogen atom parameters (Table IV(b)) as well as a listing of observed and calculated structure factor amplitudes are available.[9] In this listing the F_o values are scaled by a factor of 0.6026.

Results and Discussion

Structure of NiBPT. The most noteworthy aspect of the structure shown in Figure 1 is the high degree of planarity attained by the chelate rings. The equations[11] of two relevant mean planes along with the perpendicular displacements of the atoms are as follows. I (Ni, O, O′, N_3, N_3′): $0.7542x - 0.2962y + 0.5860z = 2.919$, Ni(0.001 Å), O(−0.012 Å), O′(−0.012 Å), N_3(0.012 Å), N_3′(0.011 Å). II (O, N_1, N_2, N_3, O′, N_1′, N_2′, N_3′): $0.7542x - 0.2973y + 0.5855z = 2.913$, Ni(−0.004 Å), O(−0.006 Å), N_1(−0.018 Å), N_2(0.010 Å), N_3(0.016 Å), O′(−0.010 Å), N_1′(−0.014 Å), N_2′(0.009 Å), N_3′(0.014 Å). It is clear that the coordinating atoms as well as the two chelate rings achieve a high degree of planarity in this complex with negligible displacement of the central metal atom from the mean planes. However, there is considerable deviation of the coordination polyhedron from square planarity, and the symmetry of coordination can at best be described as C_{2h}.

The important bond lengths and angles are given in Table V. (Not included in the tables are 18 C–H distances, average value 1.00 (4, 1) Å, and 12 H–C–H and 6 N–C–H angles, average values 108 (5, 1) and 108 (4, 1)°, respectively.)[10] The values in the halves of the molecule are equal within the uncertainties of measurement. The average values of Ni–O and Ni–N distances are 1.852 (1, 5) and 1.842 (8, 7) Å, respectively. Both these values are among the lowest reported for Ni–O and Ni–N distances. The latter closely approaches the shortest value reported for Ni–N distance, viz., 1.832 (11) Å for bis(*o*-phenylenediamino)nickel.[12]

In the triazine 1-oxide moiety, the N(2)–N(3) and N(1)–O

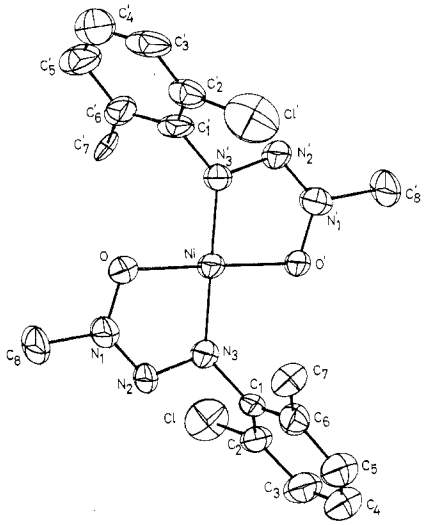

Figure 1. ORTEP diagram of the structure of NiBPT.

Table V. Important Interatomic Distances and Angles in NiBPT

(a) Distances (Å)

Ni-O	1.852 (5)	Ni-N(3)	1.837 (7)
Ni-O′	1.851 (5)	Ni-N(3′)	1.848 (7)
O-N(1)	1.341 (9)	O′-N(1′)	1.337 (9)
N(1)-N(2)	1.284 (10)	N(1′)-N(2′)	1.275 (10)
N(2)-N(3)	1.337 (9)	N(2′)-N(3′)	1.343 (9)
N(1)-C(8)	1.475 (11)	N(1′)-C(8′)	1.472 (10)
N(3)-C(1)	1.434 (10)	N(3′)-C(1′)	1.418 (11)
C(1)-C(2)	1.359 (11)	C(1′)-C(2′)	1.370 (12)
C(2)-C(3)	1.405 (10)	C(2′)-C(3′)	1.393 (14)
C(3)-C(4)	1.392 (15)	C(3′)-C(4′)	1.395 (19)
C(4)-C(5)	1.368 (15)	C(4′)-C(5′)	1.348 (16)
C(5)-C(6)	1.404 (14)	C(5′)-C(6′)	1.414 (15)
C(6)-C(1)	1.398 (13)	C(6′)-C(1′)	1.426 (14)
C(2)-Cl	1.733 (9)	C(2′)-Cl′	1.736 (12)
C(6)-C(7)	1.576 (11)	C(6′)-C(7′)	1.544 (13)

(b) Angles (deg)

O-Ni-N(3)	83.3 (3)	O′-Ni-N(3′)	83.8 (3)
O-Ni-N(3′)	96.8 (3)	O′-Ni-N(3)	96.0 (3)
Ni-O-N(1)	109.4 (5)	Ni-O′-N(1′)	108.5 (4)
O-N(1)-N(2)	120.9 (6)	O′-N(1′)-N(2′)	122.6 (6)
N(1)-N(2)-N(3)	110.9 (6)	N(1′)-N(2′)-N(3′)	110.6 (6)
N(2)-N(3)-Ni	115.4 (5)	N(2′)-N(3′)-Ni	114.5 (5)
O-N(1)-C(8)	117.4 (7)	O′-N(1′)-C(8′)	116.6 (7)
N(2)-N(1)-C(8)	121.6 (7)	N(2′)-N(1′)-C(8′)	120.8 (7)
Ni-N(3)-C(1)	132.8 (5)	Ni-N(3′)-C(1′)	133.4 (5)
N(2)-N(3)-C(1)	111.7 (6)	N(2′)-N(3′)-C(1′)	111.5 (6)
N(3)-C(1)-C(2)	121.3 (8)	N(3′)-C(1′)-C(2′)	121.1 (8)
N(3)-C(1)-C(6)	119.0 (7)	N(3′)-C(1′)-C(6′)	118.7 (8)
C(1)-C(2)-C(3)	123.0 (8)	C(1′)-C(2′)-C(3′)	122.8 (9)
C(2)-C(3)-C(4)	116.5 (8)	C(2′)-C(3′)-C(4′)	116.9 (9)
C(3)-C(4)-C(5)	121.6 (9)	C(3′)-C(4′)-C(5′)	121.6 (10)
C(4)-C(5)-C(6)	120.9 (9)	C(4′)-C(5′)-C(6′)	122.1 (11)
C(5)-C(6)-C(1)	118.2 (8)	C(5′)-C(6′)-C(1′)	115.8 (9)
C(6)-C(1)-C(2)	119.8 (8)	C(6′)-C(1′)-C(2′)	120.2 (8)
C(1)-C(2)-Cl	120.5 (7)	C(1′)-C(2′)-Cl′	118.7 (7)
C(3)-C(2)-Cl	116.4 (6)	C(3′)-C(2′)-Cl′	118.4 (8)
C(1)-C(6)-C(7)	121.4 (7)	C(1′)-C(6′)-C(7′)	122.1 (8)
C(5)-C(6)-C(7)	120.3 (8)	C(5′)-C(6′)-C(7′)	122.1 (9)

distances are equal within experimental error. The average values are, respectively, 1.340 (4, 9) and 1.339 (3, 9) Å. The N(1)–N(2) distance is appreciably shorter, average value 1.279 (6, 10) Å. This is interesting from the point of view of delocalization in the chelate ring. From the bond distances we can infer that, of the two valence bond structures I and II, the second one makes a larger contribution to the electronic structure of the triazine 1-oxide moiety. From considerations of the extent of charge separation, one might conclude that structure I should be more stable. Complexation with the central metal ion must be responsible for the greater stability

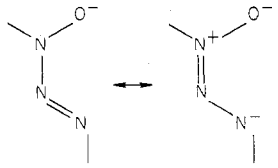

I II

of II. In this context, it will be worthwhile to determine the molecular structure of the free ligand anion. Unfortunately, no such data is available at present.

The average value of the two O–Ni–N angles is 83.5 (4, 3)°. All the six-membered ring complexes for which structural information is available have a value greater than 90° for this bond angle. The large reduction in the present case must be due to the combined effect of the smaller "bite" of the five-membered ring, the shortening of the N(1)–N(2) bond, and the short Ni–N and Ni–O distances.

The two phenyl rings are considerably twisted out of the chelate plane, the angles between the mean planes being ~81 and ~71°. Hence there is little scope for any extended conjugation. Lack of conjugation is also reflected in the C(1)–N(3) bond distances which lie within the range for a single bond value.

Another noteworthy aspect of the structure is the absence of any interaction between the chlorine atom and the central metal ion. The Ni–Cl distance is 4.103 Å, which should be compared to a value of 2.98 Å in CoBPTH,[5] where a weak cobalt–chlorine binding was suggested. CoBPTH has a highly distorted octahedral structure, with an angle of ~74° between the two chelate planes. From a close examination of its structure one can see that NiBPT or CoBPT cannot take up a similar structure because of unfavorable steric interaction between the C methyl group and the N_2 atom of the triazine 1-oxide ring. In a structure similar to that of CoBPTH, the distance between the nitrogen atom and the surface of the sphere of enclosure of the methyl group would be as small as 1.45 Å.

Isomorphism of NiBPT and CoBPT. X-ray powder photographs (taken with Cu Kα radiation by using the Debye–Scherrer technique with a camera radius of 28.65 nm) for NiBPT and CoBPT were found to be identical, proving the isomorphism of the two compounds. Isomorphism of two crystals does not necessarily mean that they are isostructural, a notable case in point being that of copper and zinc diethyldithiocarbamates.[13] However, in the present case, the cobalt complex is most likely to be isostructural with its nickel analogue for two reasons: (i) both NiBPT and CoBPT do not exhibit paramagnetic equilibrium in solution, thereby indicating absence of molecular association or tetrahedral distortion; (ii) as pointed out earlier, weak coordination of the chlorine atoms and consequent distortion of the coordination geometry is not sterically feasible in the two complexes.

Crystal Packing in NiBPT. The projection of the unit cell contents down the crystallographic *b* axis is shown in Figure 2. The crystal is made up of discrete molecules held together by van der Waals forces. The shortest intermolecular contact is between O and C_8' in the molecule translated along the *b* axis, and its value is 3.410 (10) Å. The angle between the NiN_2O_2 coordination planes of the successive molecules is 34.4°.

Structure of NiBPT·C_6H_6. An ORTEP drawing of the complex molecule and the benzene solvate is given in Figure 3. All the structurally independent bond distances and angles are given in Table VI. The structural parameters in the complex molecule are essentially same as those of NiBPT. A notable difference is that the NiN_2O_2 coordination polyhedron in the present case is constrained to be rigorously planar because of the crystallographic $\bar{1}$ symmetry. Thus the co-

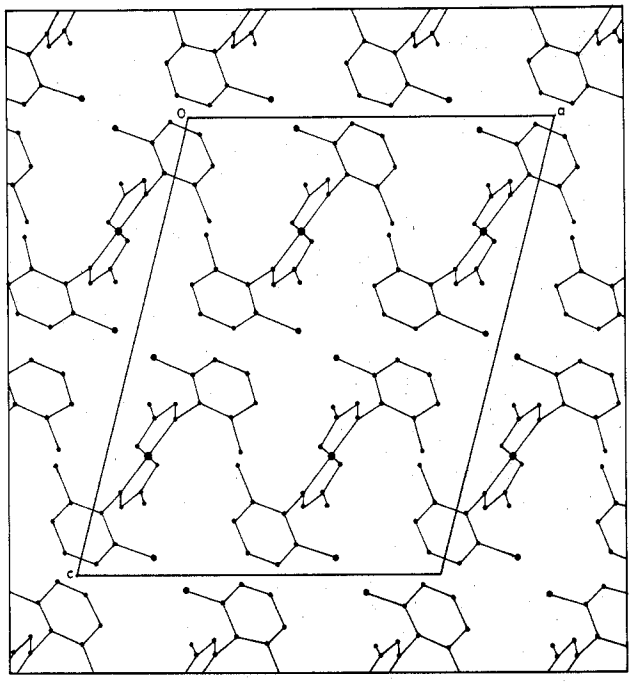

Figure 2. Structure of NiBPT shown in its *ac* plane projection.

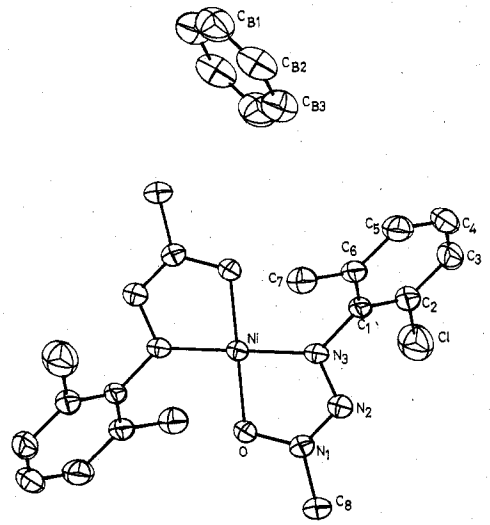

Figure 3. ORTEP diagram of a molecule of NiBPT along with its benzene solvate.

ordination has an exact C_{2h} symmetry while the whole molecule has a C_i symmetry.

The benzene molecule is situated too far away from the nickel atom to have any appreciable interaction with it, the closest contact being 3.756 Å. The dihedral angle between the benzene plane and the complex plane is 57°. The carbon atoms in the benzene solvate have the largest thermal vibration parameters, the average value of the largest principal root-mean-square amplitude being 0.315 Å, and their vibration is highly anisotropic. This is expected in view of the weak binding of the benzene molecules in the lattice which are held together only by weak van der Waals forces.

The facile decomposition of the crystal involving the loss of benzene (the deterioration is appreciable even at 0 °C) can be rationalized from the nature of the crystal packing which is shown in its *ac* plane projection in Figure 4. The crystal is made up of alternating columns of complex molecules and benzene molecules. The benzene molecules can leave the crystal along $\sim b^*$ direction without being obstructed by any part of the complex moiety. It is also interesting to note that X-ray powder patterns of NiBPT and NiBPT·C_6H_6 crystals after the loss of benzene are identical, indicating that the escape of benzene from the lattice is accompanied by triclinic to monoclinic phase transition.

Table VI. Important Interatomic Distances and Angles in NiBPT·C_6H_6

(a) Distances (Å)

Ni-O	1.843 (3)	Ni-N(3)	1.853 (3)
O-N(1)	1.357 (2)	N(1)-N(2)	1.275 (3)
N(2)-N(3)	1.318 (3)	N(1)-C(8)	1.449 (4)
N(5)-C(1)	1.443 (3)	C(1)-C(2)	1.391 (4)
C(2)-C(3)	1.391 (4)	C(3)-C(4)	1.381 (5)
C(4)-C(5)	1.403 (4)	C(5)-C(6)	1.399 (4)
C(6)-C(1)	1.399 (4)	C(2)-Cl	1.741 (4)
C(6)-C(7)	1.531 (3)	C(B1)-C(B2)	1.367 (4)
C(B2)-C(B3)	1.388 (5)	C(B3)-C(B1′)[a]	1.362 (4)

(b) Angles (deg)

O-Ni-N(3)	83.2 (1)	Ni-O-N(1)	109.1 (1)
O-N(1)-N(2)	120.9 (2)	N(1)-N(2)-N(3)	111.3 (2)
N(2)-N(3)-Ni	115.4 (2)	O-N(1)-C(8)	116.8 (2)
N(2)-N(1)-C(8)	122.1 (2)	Ni-N(3)-C(1)	132.0 (2)
N(2)-N(3)-C(1)	112.2 (2)	N(1)-C(1)-C(2)	120.6 (2)
N(1)-C(1)-C(6)	119.6 (2)	C(1)-C(2)-C(3)	121.4 (3)
C(2)-C(3)-C(4)	119.0 (3)	C(3)-C(4)-C(5)	120.1 (3)
C(4)-C(5)-C(6)	121.7 (3)	C(5)-C(6)-C(1)	117.9 (2)
C(6)-C(1)-C(2)	119.8 (2)	C(1)-C(2)-Cl	120.4 (2)
C(3)-C(2)-Cl	118.2 (2)	C(1)-C(6)-C(7)	121.0 (2)
C(5)-C(6)-C(7)	121.0 (2)	C(B1)-C(B2)-C(B3)	120.9 (3)
C(B2)-C(B3)-C(B1′)[a]	119.4 (3)	C(B3′)-C(B1′)-C(B2)[a]	119.8 (3)

[a] C(B1′) and C(B3′) are centrosymmetric equivalent of C(Bl) and C(B3), respectively.

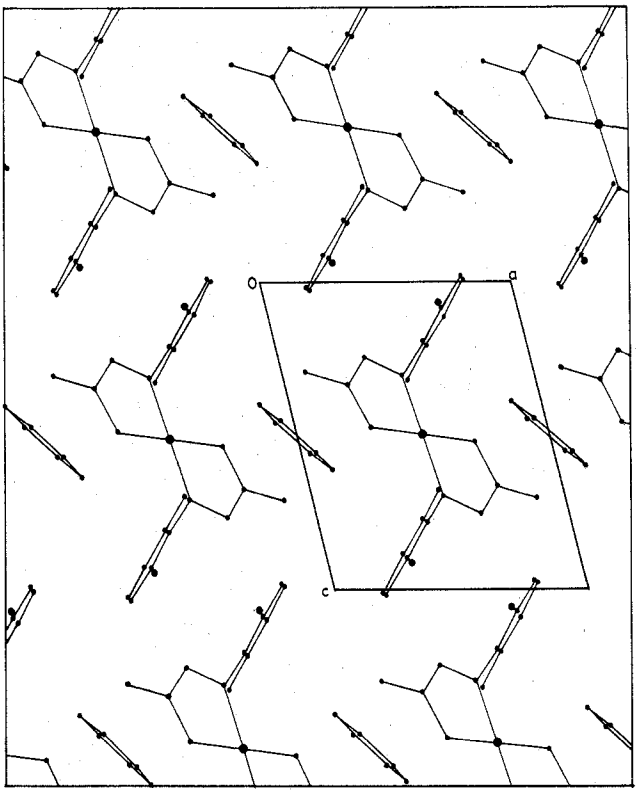

Figure 4. Structure of NiBPT·C_6H_6 shown in its *ac* plane projection.

Acknowledgment. M.V.R. gratefully acknowledges a scholarship from the National Council of Educational Research and Training (NCERT), New Delhi, during the course of this investigation. We thank the reviewers for their constructive criticism and for pointing out a few errors.

Registry No. NiBPT, 70368-88-6; NiBPT·C_6H_6, 70368-89-7.

Supplementary Material Available: A listing of the structure factor amplitudes for NiBPT and NiBPT·C_6H_6 and the hydrogen atom parameters, Tables III(b) and IV(b) (22 pages). Ordering information

is given on any current masthead page.

References and Notes

(1) Indian Institute of Technology, Madras.
(2) Indian Institute of Science, Bangalore.
(3) (a) M. Elkins and L. Hunter, *J. Chem. Soc.*, 1346 (1938); (b) D. N. Purohit, *Talanta*, **14**, 353 (1967), and references cited therein; (c) A. Chakravorty, B. Behera, and P. S. Zacharias, *Inorg. Chim. Acta*, **2**, 85 (1968); (d) B. Behera and A. Chakravorty, *J. Inorg. Nucl. Chem.*, **31**, 1791 (1969); *Inorg. Chim. Acta*, **4**, 372 (1970); (e) P. S. Zacharias and A. Chakravorty, *Inorg. Chem.*, **10**, 1961 (1971); (f) P. S. Zacharias, Ph.D. Thesis, Indian Institute of Technology, Kanpur, India, 1971.
(4) V. P. Chacko and P. T. Manoharan, *J. Magn. Reson.*, **22**, 7 (1976).
(5) G. C. Dwivedi and R. C. Srivastava, *Acta Crystallogr., Sect. B*, **27**, 2316 (1971).
(6) R. H. Holm and M. J. O'Connor, *Prog. Inorg. Chem.*, **14**, 241 (1971) (a review of the stereochemistry of bis(chelate) complexes), and references cited therein.
(7) (a) R. C. Hoy and R. H. Morriss, *Acta Crystallogr.*, **22**, 476, (1967); (b) J. Iball and C. H. Morgan, *J. Chem. Soc. A*, 52 (1967); (c) N. A. Bailey, P. M. Harrison, and R. Mason, *Chem. Commun.*, 559 (1968).
(8) Programs for the IBM 370/155 used for this work were all locally written except Johnson's ORTEP thermal ellipsoid plot program. Atomic scattering factors for all atoms were taken from "International Tables for X-ray Crystallography", Vol. III, J. S. Kasper and K. Lonsdale, Eds., Kynoch Press, Birmingham, England, 1959, p 202. Corrections for the real part of the anomalous scattering of nickel and chlorine were taken from D. T. Cromer, *Acta Crystallogr., Sect. A*, **18**, 17 (1965).
(9) Supplementary material.
(10) The first figure in parentheses following an average value is the mean deviation ($[\sum(x - \bar{x})^2/[m(m-1)]]^{1/2}$) of the average calculated over m measurements, and the second figure is the root-mean-square value of the standard deviations in individual measurements ($[\sum\sigma(x)^2/m]^{1/2}$).
(11) Equations of the least-squares planes are in the form $lx + my + nz = D$ where the coordinates, x, y, z, are in Å and are referred to a Cartesian coordinate system with $\vec{i}$ along the a axis and $\vec{j}$ along the b^* axis. D is the perpendicular distance of the mean plane from the origin.
(12) G. S. Hall and R. H. Soderberg, *Inorg. Chem.*, **7**, 2300 (1968).
(13) See, for example, R. Eisenberg, *Prog. Inorg. Chem.*, **12**, 338 (1970).

Contribution from the Institut für Physikalische und Theoretische Chemie, Tübingen, West Germany, and the Institut für Anorganische Chemie, Heidelberg, West Germany

Molecular Structures of Di-μ-oxy-diselenium Octafluoride, $Se_2O_2F_8$, and Di-μ-oxy-ditellurium Octafluoride, $Te_2O_2F_8$

HEINZ OBERHAMMER* and KONRAD SEPPELT

Received September 7, 1978

The molecular structures of $Se_2O_2F_8$ and $Te_2O_2F_8$ have been determined in the gas phase by electron diffraction. The skeleton of both molecules is a planar four-membered ring, with Se–O = 1.779 (7) Å, ∠SeOSe = 97.5 (0.5)°, Te–O = 1.918 (9) Å, and ∠TeOTe = 99.5 (0.6)°. All geometric parameters are r_g values, and error limits are 3 times the standard deviations. The configuration around the chalcogen atoms deviates considerably from octahedral with equatorial X–F bonds about 0.03–0.04 Å shorter than the axial X–F bonds. The geometric parameters and vibrational amplitudes are given.

Introduction

The structural behavior of the heavier main-group element oxyfluorides became of interest only a few years ago; e.g., many new selenium and tellurium oxyfluorides are stable and inert materials and thus are preferable compounds for structural investigations.[1-3] Soon it was found out that tellurium(VI) avoids double bonded oxygen,[2,3] whereas in the case of selenium at least two examples with Se–O double bonds are known: the stable SeO_2F_2 and the highly unstable $SeOF_4$.[4,5] The latter stabilizes by forming a dimer, $Se_2O_2F_8$.[5] The analogous tellurium oxide fluoride $Te_2O_2F_8$ was found soon afterward, although the monomeric species $TeOF_4$ has not yet been detected.

Vibrational spectroscopy and especially ^{19}F NMR spectroscopy quickly led to the four-membered ring structure of the two title molecules. This has been confirmed by repeated measurements.[6] An earlier investigation of the gas-phase structures of F_5SOSF_5, $F_5SeOSeF_5$, and $F_5TeOTeF_5$ showed results that raised the question of (pd)π bonding.[1] A comparison of the geometric parameters of the strained XO_2X skeleton with the respective parameters of $F_5X–O–XF_5$ molecules may give more detailed information about the question of (pd)π bonding in such highly oxidized species.

Experimental Section

$Se_2O_2F_8$. This compound was prepared by pyrolysis of $Na^+OSeF_5^-$ via the intermediate formation of $SeOF_4$.[5] It is often the decomposition product of many $OSeF_5$ species like $As(OSeF_5)_3$ and may be purified from such a decomposition.[7] The crude product is washed with a sodium hydroxide water solution to remove all hydrolyzable compounds and then dried over P_4O_{10}. It is distilled under dynamic vacuum several times to remove traces of SeF_6. The final physical data are mp −12 °C and bp 65 °C. The absence of SeF_6, $HOSeF_5$, $F_5SeOSeF_5$, and other impurities may be checked by ^{19}F NMR spectroscopy. $Se_2O_2F_8$ is a clear liquid with an unpleasant odor.

$Te_2O_2F_8$. A new method of preparation described as the original method[5] by pyrolysis of $Li^+OTeF_5^-$ turned out to be ineffective. Thus $B(OTeF_5)_3$[8] is sublimed at room temperature through a 600 °C quartz tube with a length of 60 cm. The products are frozen out at −196 °C. Trap to trap distillation in a glass vacuum line removes the major impurities $B(OTeF_5)_3$, TeF_6, and BF_3. (Alkaline water leads to complete hydrolysis!) The product is then dried over P_4O_{10} and again distilled under dynamic vacuum. The yield exceeds 80%.

$$B(OTeF_5)_3 \xrightarrow{600\ °C} BF_3 + {}^3/_2Te_2O_2F_8$$

$Te_2O_2F_8$ is a colorless liquid with a garlic-like smell: mp 28 °C; bp 77.5 °C.

The diffraction intensities were recorded with a Balzers Diffractograph, Model KD-G2, at two camera distances, 50 and 25 cm.[9] Kodak Electron Image plates (18 × 13 cm) were used. Details of the experiment are summarized in Table I. The electron wavelength was determined from ZnO diffraction patterns. Four plates were exposed for each camera distance, two of which were selected for the structure determination. The procedures for data analysis and background refinement are described in ref 10. The averaged modified molecular intensities for the two camera distances are shown in Figures 1 and 2. (Numerical values of the total intensities are available as supplementary material.)

Structure Analysis

Primary molecular models with D_{2h} symmetry, obtained from analysis of the radial distribution functions (Figures 3 and 4), were refined by least-squares procedures based on the molecular intensities. A diagonal weight matrix was used with

* To whom correspondence should be addressed at the Institut für Physikalische und Theoretische Chemie.

0020-1669/79/1318-2226$01.00/0